J. Fluid Mech. (2000), *vol.* 424, *pp.* 303–326. Printed in the United Kingdom

On the reflection and transmission of sound in a thick shear layer

By L. M. B. C. CAMPOS AND M. H. KOBAYASHI

Secção de Mecânica Aeroespacial, ISR, Instituto Superior Técnico Av. Rovisco Pais, 1049-001 Lisboa, Portugal

(Received 1 November 1999 and in revised form 3 July 2000)

The propagation of sound across a shear layer of finite thickness is studied using exact solutions of the acoustic wave equation for a shear flow with hyperbolic-tangent velocity profile. The wave equation has up to four regular singularities: two corresponding to the upper and lower free streams; one corresponding to a critical layer, where the Doppler-shifted frequency vanishes if the free streams are supersonic; and a fourth singularity which is always outside the physical region of interest. In the absence of a critical layer the matching of the two solutions, around the upper and lower free streams, specifies exactly the acoustic field across the shear layer. For example, for a sound wave incident from below (i.e. upward propagation in the lower free stream), the reflected wave (i.e. downward propagating in the lower free stream) and the transmitted wave (i.e. upward propagating in upper free stream) are specified by the continuity of acoustic pressure and vertical displacement. Thus the reflection and transmission coefficients, which are generally complex, i.e. involve amplitude and phase changes, are plotted versus angle of incidence for several values of free stream Mach number, and ratio of thickness of the shear layer to the wavelength; the vortex sheet is the particular case when the latter parameter is zero. The modulus and phase of the total acoustic field are also plotted versus the coordinate transverse to the shear flow, for several values of angle of incidence, Mach number and shear layer thickness. The analysis and plots in the present paper demonstrate significant differences between sound scattering by a shear layer of finite thickness, and the limiting case of the vortex sheet.

1. Introduction

There is an extensive literature on the acoustics of shear flows, dating back more than half a century (Haurwitz 1932; Kücheman 1938; Pridmore-Brown 1958; Möhring, Muller & Obermeier 1963; Nayfeh, Kaiser & Telionis 1975), which particular emphasis on boundary layers (Almgren 1976; Goldstein 1979, 1982; Myers & Chuang 1983; Hanson 1984) and shear layers (Miles 1958; Graham & Graham 1968; Balsa 1976*a*, *b*). In most of the literature the acoustic wave equation in a shear flow is solved approximately, except for two exact solutions, in the case of an homentropic linear shear (Goldstein & Rice 1963; Jones 1977, 1978; Scott 1979; Koutsoyanis 1979; Koutsoyanis, Karamcheti & Galant 1980; Campos, Oliveira & Kobayashi 1999) and an exponential shear (Campos & Serrão 1999). When a linear shear flow is matched to one or two uniform streams, to represent respectively a boundary layer or a shear layer, the velocity profile has a kink at the matching point, and thus the vorticity is discontinuous, i.e. it jumps from a constant value in the linear shear flow, to zero

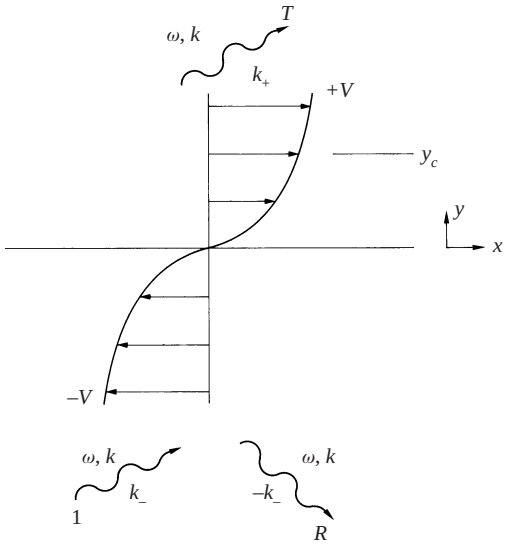

FIGURE 1. Acoustic wave with frequency ω and horizontal wavenumber k incident on a shear layer from below, giving rise to a reflected wave below and a transmitted wave above. A critical layer exists in the upper half of the shear layer for a supersonic free stream.

in the uniform stream(s) to which the linear shear is matched. The present paper considers a shear layer with an hyperbolic-tangent velocity profile (figure 1), for which both the velocity and vorticity are smooth functions, the former monotonically increasing between the two free streams, and the latter monotonically decreasing from the mid-line. The hyperbolic-tangent shear flow profile has been studied before (Michalke 1965) from the point of view of inviscid stability theory (Lin 1955; Drazin & Reid 1979; Michalke 1984).

The acoustic wave equation (§ 2) in a hyperbolic-tangent shear flow (§ 2.1) has three singularities (§ 2.2) in the flow domain: at the free streams, and at a critical layer, where the Doppler-shifted frequency vanishes. In the case of a shear layer, without a critical layer, only the two pairs of solutions about the two free streams are needed and they are distinct in the upper (§ 2.3) and lower (§ 3.1) free streams, because the mean flow velocity is reversed. Their matching in the shear layer, to ensure continuity of the acoustic pressure and normal displacement, specifies (§ 3.2) the reflection and transmission coefficients, e.g. for a wave incident from below, with the vortex sheet as limiting (case) of zero thickness. In the presence of a critical layer, a third pair of solutions would be needed for a shear layer, to match to the solutions around the free streams, which are valid only up to the critical layer; in this way the wave field can be extended across the whole shear layer, and continuity of pressure and displacement can be used again to determine the scattering (reflection and transmission) coefficients. The remaining case is that of acoustic propagation at the Mach condition $M \cos\theta = 1$, for which the critical layer lies in the upper free stream; it can be shown (§ 3.3) that the acoustic field consists of asymptotically evanescent and divergent components. The latter can be eliminated for a shear layer, but only with a particular choice of reflection and transmission coefficients. The relation of the present problem of sound propagation in a shear layer to the triggering of shear layer instabilities by sound is discussed briefly (Appendix A); both problems can use the same series solutions, whose rate of convergence and truncation properties are also mentioned (Appendix B).

The scattering of sound in a shear layer depends on five parameters: wave frequency ω, wavelength in the free stream λ, sound speed c, free-stream velocity V and 'thickness' L of the shear flow. With these five parameters, three dimensionless parameters can be formed, i.e. the angle of incidence θ, Mach number M of the free stream and 'thickness' of the shear layer $\delta = L/\lambda$ normalized to the wavelength in the free stream. Thus the scattering coefficients (for reflection R or transmission T) depend on the angle of incidence θ, and also on Mach number M and thickness δ. The limit $\delta \to 0$ represents a vortex sheet (Miles 1958), and the opposite limit $\delta \to \infty$, sound 'rays' (Amiet 1978), is a slowly varying shear flow; the most interesting case $\delta \sim 1$ is sound scattering by a shear layer of 'finite thickness' on a wavelength scale. The present analysis covers the whole range of shear flow thickness δ and Mach number M (§4.1), both for the calculation of scattering coefficients (§4.2) and the acoustic pressure (§4.3), including supersonic shear layers (§5) for which $M\cos\theta \geqslant 1$ and thus a critical layer exists. Other aspects of the problem concern sound radiation by sources near a shear flow (Ffowcs Williams 1974) and the triggering of instabilities (Michalke & Timme 1967; Michalke 1989).

2. Sound propagation in the hyperbolic-tangent shear flow profile

The two-dimensional propagation of sound in an unidirectional shear flow, with an hyperbolic-tangent profile, is studied starting from the acoustic wave equation in an unidirectional shear flow (§2.1), and considering its singularities at (§2.2) a critical layer and in (§2.3) the free streams. The matching of solutions around these singularities specifies the acoustic field in the whole flow region, including the asymptotic forms in the free streams.

2.1. *Acoustic wave equation for unidirectional shear flow*

Consider (figure 1) a unidirectional shear flow with hyperbolic-tangent profile:

$$\boldsymbol{U}(y) = V\tanh(y/L)\boldsymbol{e}_x. \tag{1}$$

This represents a smooth velocity profile between $\mp V$ at $\mp\infty$:

$$\boldsymbol{U}(y \to \pm\infty) = \pm V[1 \mp 2\mathrm{e}^{\mp 2y/L} + O(\mathrm{e}^{\mp 4y/L})]\boldsymbol{e}_x, \tag{2a}$$

and vorticity:

$$\boldsymbol{q} \equiv \nabla \wedge \boldsymbol{U} = -(V/L)\mathrm{sech}^2(y/L)\boldsymbol{e}_x, \tag{2b}$$

which varies from $-V/L$ at $y = 0$ to zero at $y = \pm\infty$. The case of distinct free-stream velocities:

$$\boldsymbol{U}(-\infty) = U_1, \quad U(+\infty) = U_2, \tag{3a,b}$$

reduces to

$$V = (U_2 - U_1)/2, \quad U_0 = (U_2 + U_1)/2, \tag{4a,b}$$

in a reference frame moving at velocity U_0, i.e. the Doppler-shifted frequency

$$\omega_0 = \omega - kU_0 \tag{4c}$$

is used instead of ω.

Since the mean state does not depend on time t and horizontal coordinate x, it is convenient to use the Fourier representation of the two-dimensional acoustic pressure field

$$p(x,y,t) = \iint_{-\infty}^{+\infty} P(y;k,\omega)\mathrm{e}^{\mathrm{i}(kx-\omega t)}\,\mathrm{d}k\,\mathrm{d}\omega, \tag{5}$$

where $P(y;k,\omega)$ is the acoustic pressure perturbation spectrum for a wave of frequency ω and horizontal wavenumber k, at transverse position y. It satisfies the acoustic wave equation in a unidirectional shear flow (Campos & Kobayashi 2000*a*):

$$P''+2[c'/c+kU'/(\omega-kU)]P'+[(\omega-kU)^2/c^2-k^2]P=0, \tag{6}$$

where a prime denotes derivative with respect to y, e.g. $P'\equiv \mathrm{d}P/\mathrm{d}y$, and c is the adiabatic sound speed of the mean flow

$$c^2=(\partial p_0/\partial\rho_0)_s. \tag{7}$$

The unidirectional shear flow corresponds to uniform mean flow pressure p_0, and in (7) it is assumed that the mean flow is isentropic, i.e. $\mathrm{d}s/\mathrm{d}t=0$, where $\mathrm{d}/\mathrm{d}t\equiv\partial/\partial t+U\partial/\partial x$ is the material derivative. If the mean flow is assumed to be homentropic $s_0=$ const, then the equation of state $p_0=p_0(\rho_0,s_0)$ implies constant mean flow mass density $\rho_0=$ const, and constant sound speed $c=0$, so that the acoustic wave equation (6) simplifies in a homentropic unidirectional shear flow to

$$(1-kU/\omega)P''+2(k/\omega)U'P'+k^2(1-kU/\omega)[(1-kU/\omega)^2(\omega/kc)^2-1]P=0, \tag{8}$$

the usual form in the literature (Haurwitz 1932; Kücheman 1938; Pridmore-Brown 1958; Möhring *et al.* 1963; Campos & Serrão 1999).

When introducing the hyperbolic-tangent shear flow profile (1) in the wave equation (8), it is convenient to make the change of independent variable:

$$\xi\equiv\tanh(y/L),\quad \Phi(\xi)\equiv P(y;k,\omega), \tag{9a,b}$$

leading to a linear second-order differential equation with polynomial coefficients:

$$(1-\Lambda\xi)(1-\xi^2)^2\Phi''+2(1-\xi^2)(\Lambda-\xi)\Phi'+(1-\Lambda\xi)[\Omega^2(1-\Lambda\xi)^2-K^2]\Phi=0, \tag{10}$$

where a prime denotes derivative with respect to ξ, and three dimensionless parameters appear:

$$\Omega\equiv\omega L/c,\quad K\equiv kL,\quad \Lambda\equiv kV/\omega. \tag{11a,b,c}$$

The first parameter (11*a*) appears as a dimensionless 'frequency':

$$\Omega=2\pi L/\tau c=2\pi L/\lambda=2\pi\delta,\quad \delta\equiv L/\lambda, \tag{12a,b}$$

where the wave period $\tau=2\pi/\omega$, and wavelength $\lambda=\tau c$ have been introduced; this parameter specifies the ratio of the lengthscale of the shear flow L to the wavelength of sound in the free stream λ, so $\Omega\ll 1$ or $\lambda\gg L$ corresponds to sound scattering by a 'vortex sheet', whereas $\Omega^2\gg 1$ corresponds to the 'ray limit' of a short wave in a slowly varying mean flow $\lambda\ll L^2$, with $\Omega\sim 1$ leading to the more interesting case of interaction of sound with a shear layer of 'finite' thickness. Taking the horizontal wavenumber for a medium at rest:

$$k=(\omega/c)\cos\theta, \tag{13a}$$

where θ is the angle of the direction of propagation with the mean flow, the second parameter, (11*b*), which appears as 'dimensionless wavenumber':

$$K=(\omega L/c)\cos\theta=\Omega\cos\theta, \tag{13b}$$

relative to (12*a*), specifies the direction of propagation, namely oblique for $K<\Omega$, horizontal for $K=\Omega$, with evanescent waves corresponding to $K>\Omega$. The last

Case Critical layer:	A in shear layer	B in free stream	C absent
y_c	$< \infty$	$= \infty$	imaginary
$\Lambda = M\cos\theta$	> 1	$= 1$	< 1
$M_r \equiv 1 - M\cos\theta$	< 0	$= 0$	> 0

TABLE 1. Existence and location of critical layer.

Case Critical layer:	A in shear layer	B in free stream	C absent
ξ_c	< 1	$= 1$	> 1
singularities in $(-1,+1)$	$\pm 1, \xi_c$	± 1	± 1
Radius of convergence of solution in powers of			
$1 - \xi$	$1 - \xi_c$	2	$\min\{2, \lvert 1 - \xi_c\rvert\}$
$1 + \xi$	$1 + \xi_c$	2	$\min\{2, \lvert 1 + \xi_c\rvert\}$
$1 - \Lambda\xi$	$1 - \xi_c$	(2)	$\min\{\lvert 1 - \xi_c\rvert, \lvert 1 + \xi_c\rvert\}$

TABLE 2. Solutions of the acoustic wave equation.

parameter, (11*c*),

$$\Lambda = (V/c)\cos\theta = M\cos\theta, \quad M \equiv V/c, \tag{14a,b}$$

involves the Mach number of the free stream, and in related to the Doppler factor, as will be seen next.

2.2. *Existence of a critical layer and matching of the wave fields*

The preceding account makes clear that the scattering of sound by a shear layer depends on three parameters (11*a*, *b*, *c*), which are combinations of the Mach number M, angle of incidence θ and shear layer thickness δ. The first two apply to a 'vortex sheet', and the last distinguishes a shear layer of 'finite thickness', allowing for new flow–acoustic interaction effects. The acoustic wave equation (8) has a singularity where the Doppler-shifted frequency

$$\omega_*(y) = \omega - kU(y) = \omega - kV\tanh(y/L) \tag{15a}$$

vanishes, and this determines the position y_c of the critical layer, which is specified by

$$\omega_*(y_c) = 0 : \xi_c \equiv \tanh(y_c/L) = \omega/kV = 1/\Lambda = 1/(M\cos\theta). \tag{15b}$$

If the Doppler-shifted frequency in the free stream $\omega_*(\infty) = \omega - kV < 0$ is negative, then since it is positive at the mid-line $\omega_*(0) = \omega$, it must vanish in between, at the critical layer: this is case A in table 1. If the Doppler-shifted frequency is positive in the free stream, it is positive everywhere, and no critical layer exists (case C), i.e. y_c is imaginary (15*b*) for $\Lambda < 1$. The intermediate case $\Lambda = 1$ corresponds (case B) to a critical layer in the free stream $y_c = \infty$.

It is clear that the differential equation (10) has regular singularities at

$$\xi = \pm 1, 1/\Lambda \equiv \xi_c, \quad y = \pm\infty, y_c, \tag{16a,b}$$

corresponding to the free streams and critical layer (16*b*). Exact solutions of the

Case	i	ii	iii
Condition	$\omega - kV > kc$	$\omega + kV > kc > \omega - kV$	$\omega + kV < kc$
Wavefield			
Above shear layer	Propagating	Evanescent	Evanescent
Below shear layer	Propagating	Propagating	Evanescent

TABLE 3. Conditions for wave propagation and evanescence.

acoustic wave equation can be obtained by expanding in power series around the singularities, with radius of convergence limited by the nearest singularity. There are three cases, depending on (table 1) whether a critical layer exists or not, and where it is located, according to the table 2. Thus matching of three pairs of solutions is needed only if the critical layer lies in the shear flow (case A). If the critical layer does not exist, the third singularity is beyond the unit circle, so matching of two pairs of solutions is sufficient (case C). This is also true in the case of the critical layer in the free stream (case B), because two singularities coincide $\xi_c = 1$, and the wave equation (10) simplifies to

$$\Lambda = 1: \quad (1-\xi^2)^2\Phi'' + 2(1-\xi^2)\Phi' + [\Omega^2(1-\xi)^2 - K^2]\Phi = 0, \tag{17}$$

which has only two singularities.

In the preceding discussion the singularity of the differential equation (10) at infinity $\zeta = \infty$ was not mentioned, because it lies outside the physical region at $y = i\pi/2$, and the pair of solutions in its neighbourhood is not needed to specify the acoustic field in the physical region: for completeness it is noted that the change of variable:

$$z \equiv 1/\zeta, \quad \Psi(z) \equiv \Phi(\zeta), \tag{18a,b}$$

transforms the differential equation (10) to

$$(z-\Lambda)(z^2-1)^2z^2\Psi'' + 2(z^2-1)[z^3 + \Lambda(1-2z^2)]z\Psi' + (z-\Lambda)[\Omega^2(z-\Lambda)^2 - K^2z^2]\Psi = 0, \tag{19}$$

and shows that the origin $z = 0$ is a regular singularity of (19), and thus the point at infinity $\xi = \infty$ is a regular singularity of (10). It is noted in passing that since the differential equation (10) has four regular singularities, it must be reducible to Heun's equation (Kamke 1944; Ronveaux 1996). For the acoustic problem at hand, direct solution of the differential equation (10) by the Frobenius–Fuchs method is more illuminating physically.

2.3. *Asymptotic and exact wave fields*

The asymptotic wave fields in the free streams can be readily determined because the wave equation (8) then has constant coefficients:

$$U(\pm\infty) = \pm V: \quad P'' + [(\omega \mp kV)/c^2 - k^2]P = 0. \tag{20}$$

Introducing the vertical wavenumber, respectively above k_+ and below k_- the shear layer:

$$k_\pm \equiv \left|(\omega \mp kV)^2/c^2 - k^2\right|^{1/2} = (\omega/c)\left|(1 \mp M\cos\theta)^2 - \cos^2\theta\right|^{1/2}, \tag{21}$$

the asymptotic wave fields are given by

$$P(y \to \pm\infty) \sim \begin{cases} A_\pm \exp(\mathrm{i}k_\pm y) + B_\pm \exp(-\mathrm{i}k_\pm y) & \text{if } \Delta > 0 \quad (22a) \\ A_\pm y + B_\pm & \text{if } 0 = \Delta \equiv (\omega \mp kV)^2 - k^2c^2 \quad (22b) \\ A_\pm \exp(k_\pm y) + B_\pm \exp(-k_\pm y) & \text{if } \Delta < 0, \quad (22c) \end{cases}$$

where $A_\pm, B_\pm$ are arbitrary constants of integration, to be determined from boundary or radiation conditions. It is possible to have propagating (22*a*), evanescent (22*c*) or marginal (22*b*) wave fields, above or below the shear layer in the combinations shown in table 3, which divide the frequency spectrum into three ranges separated by $\omega_\pm \equiv k(c \pm V)$.

As a first example the exact wave field near the upper free stream is obtained by expansion about $y = \infty$ or $\xi = 1$, using the variable

$$\zeta \equiv 1 - \xi, \quad F(\zeta) \equiv \Phi(\xi), \qquad (23a, b)$$

which transforms the differential equation (10) to

$$\zeta^2(2-\zeta)^2(1-\Lambda+\Lambda\zeta)F'' + 2\zeta(2-\zeta)(1-\Lambda-\zeta)F' + (1-\Lambda+\Lambda\zeta)[\Omega^2(1-\Lambda+\Lambda\zeta)^2 - K^2]F = 0. \qquad (24a)$$

Since $\zeta = 0, \xi = 1, y = +\infty$ is a regular singularity, solutions exist as Frobenius–Fuchs series:

$$F(\zeta) = \sum_{n=0}^{\infty} a_n(\sigma)\zeta^{n+\sigma}. \qquad (24b)$$

with index σ and coefficients a_n to be determined. Substitution of (24*b*) into (24*a*) leads to the follwing recurrence formula for the coefficients:

$$\begin{aligned} &(1-\Lambda)[4(n+\sigma)^2 + k_+^2L^2]a_n(\sigma) \\ &\quad = \{2(n+\sigma-1)[2(1-2\Lambda)(n+\sigma-2)+3-\Lambda] - \Lambda[k_+^2L^2 + 2\Omega^2(1-\Lambda)^2]\}a_{n-1}(\sigma) \\ &\qquad -\{(n+\sigma-2)[(1-5\Lambda)(n+\sigma-3)+2] + 3\Omega^2\Lambda^2(1-\Lambda)\}a_{n-2}(\sigma) \\ &\qquad -\Lambda\{(n+\sigma-3)(n+\sigma-4) + \Omega^2\Lambda^2\}a_{n-3}(\sigma); \end{aligned} \qquad (25a)$$

setting $n = 0$ yields

$$n = 0: \quad 0 = 4\sigma^2 + k_+^2L^2 = 4(\sigma - \sigma_+)(\sigma - \sigma_+), \qquad (25b)$$

as the indicial equation.

The indices, which are the roots of (25*b*), are specified by (21), the vertical wavenumber in the upper free stream:

$$\sigma_\pm = \mp\mathrm{i}k_+L/2. \qquad (26)$$

The variable (23*a*), (9*a*)

$$\zeta = 1 - \tanh(y/L) = 2/(1 + \mathrm{e}^{2y/L}), \qquad (27a)$$

is given asymptotically by

$$\zeta = 2\mathrm{e}^{-2y/L}[1 + O(\mathrm{e}^{-2y/L})]. \qquad (27b)$$

Thus the wavefields (24*b*)

$$a_0(\sigma_\pm) \equiv 1: \quad F_\pm(\zeta) = \sum_{n=0}^{\infty} a_n(\sigma_\pm)\zeta^{n+\sigma_\pm} \tag{28a}$$

correspond to

$$P_\pm(y) \equiv \sum_{n=0}^{\infty} a_n(\mp \mathrm{i}k_+L/2)[1-\tanh(y/L)]^{n\pm \mathrm{i}k_+L/2}, \tag{28b}$$

and have leading asymptotic terms

$$P_\pm(y \to \infty) \sim \zeta^{\sigma_\pm} \sim \mathrm{e}^{-2\sigma_\pm y/L} \sim \mathrm{e}^{\pm \mathrm{i}k_+ y}, \tag{29a}$$

respectively upward P_+ and downward P_- propagating waves, in agreement with (22*a*). The total acoustic field is thus given by

$$P(y) = A_+P_+(y) + B_+P_-(y), \tag{29b}$$

where A_+, B_+ are arbitrary constants. In the free stream (29*b*) splits into upward and downward propagating waves (29*a*); in the shear layer, each of $P_\pm(y)$ has upward and downward propagating components, as would result from taking a spatial Fourier spectrum of (28*b*); the reason is that there are multiple partial reflections of sound in the shear layer, and since (28*b*) is exact, it includes multiple internal scattering of all orders. Thus $P_\pm(y)$ are the exact (28*b*) wave fields in the shear layer which match to respectively upward and downward propagating waves (29*a*) in the upper free stream.

3. Application to the acoustics of shear layers and vortex sheets

The hyperbolic-tangent shear flow profile is used to represent (figure 1) a shear layer. The solution around the lower free stream can be obtained (§ 3.1) similarly to that about the upper free stream (§ 2.3). In the absence of a critical layer, the two solutions are valid in overlapping regions, and the continuity of pressure and displacement specifies the scattering (reflection and transmission) coefficients for an incident acoustic field. The limiting case of zero thickness on a wavelength scale leads (§ 3.2) to the known results for the scattering of sound by a vortex sheet. When a critical layer is present in the shear layer, the matching of three solutions is necessary (table 2), except if the critical layer is the upper free stream, when again only two solutions need to be matched (§ 3.3); in this case the solution around the upper free stream is different from that obtained before in § 2.3, because the free stream coincides with the critical layer.

3.1. *Matching wave fields on two sides of the shear layer*

The exact solution (29*b*), (28*b*) applies to the sound field in the shear layer and in the absence of a critical layer it holds for $-\infty < y \leqslant +\infty$, i.e. it excludes the lower stream, which is another singularity of the wave equation. Thus it is necessary to match to the solution of the wave equation around the singularity $y = -\infty, \xi = -1$ or $\eta = 0$, where η is the new variable

$$\eta \equiv 1 + \xi, \quad G(\eta) = \Phi(\xi), \tag{30a,b}$$

which transforms the differential equation (10) to

$$\eta^2(2-\eta)^2(1+\Lambda-\Lambda\eta)G'' + 2\eta(2-\eta)(1+\Lambda-\eta)G' + (1+\Lambda-\Lambda\eta)[\Omega^2(1+\Lambda-\Lambda\eta)^2 - K^2]G = 0. \tag{31}$$

Since $\eta = 0$ is a regular singularity, there are solutions as Frobenius–Fuchs expansions:

$$G(\eta) = \sum_{n=0}^{\infty} b_n(\mu)\eta^{n+\mu}, \tag{32}$$

with index μ and coefficients b_n to be determined. Substitution of (32) into (31) yields the recurrénce formula for the coefficients:

$$\begin{aligned}(1+\Lambda)[4(n+\mu)^2 + k_-^2L^2]b_n(\mu) \\ = \{\Lambda[k_-^2L^2 + 2\Omega^2(1+\Lambda)^2] + 2(n+\mu-1)[3+\Lambda+2(1+2\Lambda)(n+\mu-2)]\}b_{n-1}(\mu) \\ -\{\Omega^2\Lambda^2(1+\Lambda) + (n+\mu-2)[2+(1+5\Lambda)(n+\mu-3)]\}b_{n-2}(\mu) \\ +\Lambda[(n+\mu-3)(n+\mu-4) + \Omega^2\Lambda^2]b_{n-3}(\mu),\end{aligned} \tag{33}$$

which is of comparable complexity to (25*a*) for the 'upper solution'.

Since the critical layer is at an unsymmetrical position $y = y_c > 0$, the upper and lower wave fields are not symmetric; nevertheless, the indicial equation, which follows from (33),

$$n = 0: \quad 0 = 4\mu^2 + k_-^2L^2 = (\mu - \mu_-)(\mu - \mu_+), \tag{34}$$

is similar to (26), i.e. has similar roots:

$$\mu_\pm = \pm \mathrm{i}k_-L/2, \tag{35}$$

with the lower vertical wavenumber k_- appearing instead of the k_+ in (21). The variable (30*a*), (9*a*)

$$\eta = 1 + \tanh(y/L) = 2/(1 + \mathrm{e}^{-2y/L}), \tag{36a}$$

scales as

$$y \to -\infty: \quad \eta = -2\mathrm{e}^{2y/L}[1 + O(\mathrm{e}^{2y/L})], \tag{36b}$$

and thus the leading terms of (32)

$$b_0 \equiv 1: \quad G_\pm(\eta) = \sum_{n=0}^{\infty} b_n(\pm \mathrm{i}k_-L/2)\eta^{n \pm \mathrm{i}k_-L/2}, \tag{37a}$$

scale as upward and downward propagating waves:

$$G_\pm(\eta) \sim (\eta)^{\pm \mathrm{i}k_-L/2} \sim \mathrm{e}^{\pm \mathrm{i}k_-}, \tag{37b}$$

in agreement with (22*a*).

Thus the wave fields below the shear layer are given by

$$P(y) = A_-P^+(y) + B_-P^-(y), \tag{38}$$

where A_-, B_- are arbitrary constants, and

$$P^\pm(y) = \sum_{n=0}^{\infty} b_n(\pm \mathrm{i}k_-L/2)[1 + \tanh(y/L)]^{n \pm \mathrm{i}k_-L/2}. \tag{39}$$

For example, a wave of unit amplitude incident from below corresponds to P^+:

$$-\infty \leqslant y < \infty: \quad P(y) = P^+(y) + RP^-(y), \tag{40}$$

and the reflection coefficient R affects the downward propagating wave P^-; the wave field (40) corresponds to (38) with $A_- = 1, B_- = R$. Above the shear layer (29*b*) there

should be an upward propagating wave $B_+ = 0$, with amplitude $A_+ = T$ equal to the transmission coefficient:

$$-\infty < y \leqslant +\infty : \quad P(y) = TP_+(y). \tag{41}$$

The wave fields (40), (41) are valid in overlapping regions, and their matching specifies the reflection R and transmission T coefficients.

3.2. *Comparison of the vortex sheet and the shear layer*

The matching of the wave fields ensures the continuity of pressure p and vertical displacement γ, which are related by the y-component of the momentum equation

$$\rho(\partial/\partial t + U\partial/\partial x)^2\gamma + \partial p/\partial y = 0. \tag{42}$$

Introducing the spectrum of the vertical displacement:

$$\gamma(x, y, t) = \iint_{-\infty}^{+\infty} \Gamma(y; k, \omega)\mathrm{e}^{\mathrm{i}(kx-\omega t)}\,\mathrm{d}k\,\mathrm{d}\omega. \tag{43a}$$

leads, (5), to the polarization relation:

$$\mathrm{d}P/\mathrm{d}y = \rho(\omega - kU)^2\Gamma = \rho\omega_*^2\Gamma, \tag{43b}$$

where the Doppler-shifted frequency (15a) is continuous. Thus P and $\mathrm{d}P/\mathrm{d}y$ are continuous, i.e. matching (40) and (41) at $y = 0$ yields

$$TF_+(1) = G_+(1) + RG_-(1), \quad -TF'_+(1) = G'_+(1) + RG'_-(1), \tag{44a, b}$$

which can be solved:

$$[F_+(1)G'_-(1) + F'_+(1)G_-(1)]\{R, T\}$$
$$= \{-F_+(1)G'_+(1) - F'_+(1)G_+(1), G_+(1)G'_-(1) - G'_+(1)G_-(1)\}. \tag{45}$$

for the reflection and transmission coefficients. The vanishing of the terms in the square brackets on the left-hand side of (45) is related to the triggering of instabilities of the shear flow by sound (Appendix A).

In the case of a shear layer of zero thickness, or a vortex sheet, the acoustic pressure is given (40), (41) exactly by the asymptotic forms (37b), (29a):

$$P(y \leqslant 0) = \mathrm{e}^{\mathrm{i}k_-y} + R_0\mathrm{e}^{-\mathrm{i}k_-y}, \quad P(y \geqslant 0) = T_0\mathrm{e}^{\mathrm{i}k_+y}, \tag{46a, b}$$

and the corresponding displacements (43b) by

$$\Gamma(y \leqslant 0) = \{\mathrm{i}k_-/[\rho(\omega + kV)^2]\}(\mathrm{e}^{\mathrm{i}k_-y} - R_0\mathrm{e}^{-\mathrm{i}k_-y}), \tag{47a}$$

$$\Gamma(y \geqslant 0) = \{\mathrm{i}k_+/[\rho(\omega - kV)^2]\}T_0\mathrm{e}^{\mathrm{i}k_+y}. \tag{47b}$$

Continuity of P and Γ at $y = 0$ yields

$$1 + R_0 = T_0, \quad k_-(1 - R_0)/(\omega + kV)^2 = k_+T_0/(\omega - kV)^2, \tag{48a, b}$$

which can be solved for the reflection and transmission coefficients of a vortex sheet:

$$R_0 = (\mu - 1)/(\mu + 1), \quad T_0 = 2\mu/(1 + \mu), \tag{49a, b}$$

where

$$\mu = (k_-/k_+)[(1 - M\cos\theta)/(1 + M\cos\theta)]^2. \tag{50}$$

In the absence of a vortex sheet $M = 0$, then $k_+ = k_-$ in (21), $\mu = 1$ in (50), and there would be total transmission $R_0 = 0$, $T_0 = 1$.

The reflection and transmission coefficients for a vortex sheet (49*a*, *b*), (50) depend only on the angle of incidence θ and Mach number M:

$$R_0, T_0(\theta; M) = \lim_{\delta \to 0} R, T(\theta; M, \delta), \tag{51}$$

and are the limit of those of the shear layer (45), for zero thickness (12*b*) and real angle of incidence $0 < \theta \leqslant \pi$; k is always real (21) in the case of acoustic waves (see Appendix A for instabilities) but k_+ is real only if

$$1 - M\cos\theta > \cos\theta \quad \text{or} \quad 1 - M\cos\theta < -\cos\theta, \tag{52a, b}$$

which implies

$$\cos\theta < 1/(M+1) \quad \text{or} \quad \cos\theta > 1/(M-1), \tag{53a, b}$$

so that sound propagates in the upper free stream if

$$\pi \geqslant \theta > \theta_+ \equiv \arg\cos[1/(1+M)] \quad \text{or} \quad 0 \leqslant \theta < \theta_- = \arg\cos[1/(M-1)]. \tag{54a, b}$$

Note that the first condition (54*a*) specifies a 'zone of silence' $\theta < \theta_+$ for all $M > 0$, whereas (54*b*) shows that for $M > 2$ the 'zone of silence' is $\theta_- < \theta < \theta_+$. A similar reasoning shows that below the shear layer k_- is real, i.e. propagating waves exist in the lower free stream if

$$0 \leqslant \theta < \pi - \theta_+ \quad \text{or} \quad \pi - \theta_+ < \theta \leqslant \pi, \tag{55a, b}$$

the first condition (55*a*) specifies a zone of silence $\pi - \theta_+ < \theta \leqslant \pi$ for all $M > 0$, and the second condition (55*b*) shows that for $M > 2$ the 'zone of silence' is $\pi - \theta_+ < \theta < \pi - \theta_-$. The situation is illustrated in figure 2, where it is shown in figure 2(*a*) that if the Mach number of the free stream is less than 2 acoustic waves can propagate on both sides of the shear layer if $\theta_+ < \theta < \pi - \theta_+$, and for $0 < \theta < \theta_+$ are evanescent above and propagating below, and for $\pi - \theta_+ < \theta < \pi$ are evanescent below and propagating above. In figure 2(*b*) it is shown that if the Mach number of the free stream is more than 2, $M > 2$, then acoustic waves can propagate on both sides of the shear layer in three arcs ($0 < \theta < \theta_-$ and $\theta_+ < \theta < \pi - \theta_+$ and $\pi - \theta_- < \theta < \pi$), and for $\theta_- < \theta < \theta_+$ are evanescent above and propagating below and for $\pi - \theta_+ < \theta < \pi - \theta_-$ are propagating above and evanescent below. The critical layer corresponds (table 1) to the angle

$$\theta_* \equiv \arg\cos(1/M), \quad \theta_- < \theta_* < \theta_+, \tag{56a, b}$$

so it exists only for a supersonic free stream $M > 1$, and lies always (56*b*) in the 'zone of silence' of the upper stream, as shown in figure 2(*a*, *b*).

3.3. *Acoustic waves at the Mach condition*

In case B, that of the acoustic field at the Mach condition $M\cos\theta = 1$, the wave equation simplifies to (17), which has only two singularities. The solution (38) at the lower stream remains valid (39), (33), with the simplification $\Lambda = 1$, and extends up to the upper stream $-\infty \leqslant y < \infty$. The solution in the upper stream (29*b*) is modified from (28*a*) as can be seen from the recurrence relation (25*a*), which fails for $\Lambda = 1$. The reason is that in case B two singularities coincide at $\xi = 1$, namely the free stream $\xi = 1$ and the critical layer $\xi_c = 1/\Lambda$ with $\Lambda = 1$ (see (16*a*)). Thus it is necessary to start with the wave equation (17), although the change of variable (23*a*, *b*) remains relevant,

$$\Lambda = 1: \quad \zeta \equiv 1 - \xi, \quad \Phi(\xi) \equiv J(\zeta) \equiv Q(y; k, kV), \tag{57a, b}$$

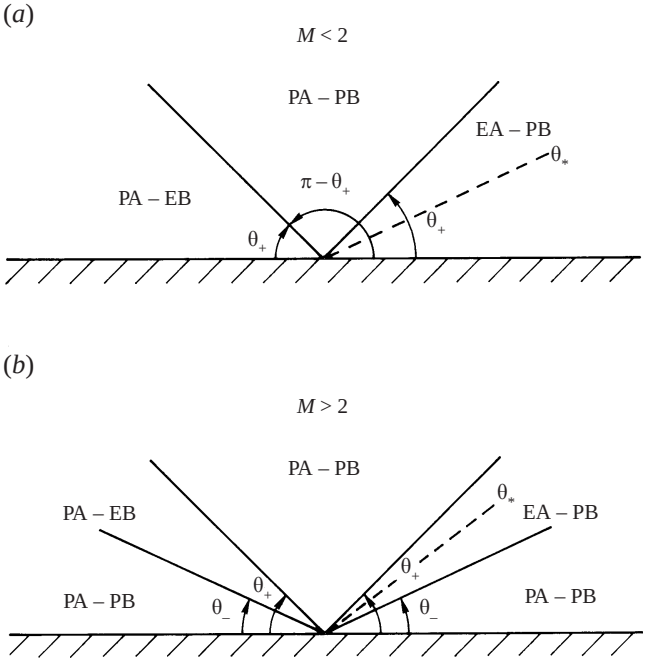

FIGURE 2. Ranges of angle of incidence for free stream Mach numbers (*a*) $M < 2$ and (*b*) $M > 2$, for which the acoustic fields are propagating (P) or evanescent (E), either above (A) or below (B) the shear layer, in terms of the angles $\theta_{\pm}$ in (54*a*, *b*). The angle of incidence θ_* (56*a*) corresponding to the critical layer is also indicated.

with $k = (\omega/c)\cos\theta = (\omega/c)(\Lambda/M)$ from (13*a*), (14*a*), so that $\omega = kV$ for $\Lambda = 1$. The differential equation is thus

$$\zeta^2(2-\zeta)^2 J'' - 2\zeta(2-\zeta)J' + (\Omega^2\zeta^2 - K^2)J = 0, \tag{58}$$

which is simpler than in the general case (24*a*), from which it can be obtained by setting $\Lambda = 1$.

When the critical layer lies in the upper free stream, it remains a regular singularity, so that solutions exist in the form

$$J(\zeta) = \sum_{n=0}^{\infty} f_n(\nu)\zeta^{n+\nu}, \tag{59}$$

with recurrence formula for the coefficients:

$$[4(n+\nu)(n+\nu-2) - K^2]f_n(\nu) = 2(n+\nu-1)(2n+2\nu-3)f_{n-t}(\nu) - [(n+\nu-2)(n+\nu-3) + \Omega^2]f_{n-2}(\nu). \tag{60}$$

Setting $n = 0$ yields

$$n = 0: \quad 0 = 4\nu(\nu-2) - K^2 \tag{61}$$

as the indicial equation. Of the two indices

$$\nu_+ > 0 > \nu_-: \quad \nu_{\pm} = 1 \pm \sqrt{1 + K^2/4}, \tag{62}$$

M	θ_-	θ_+	$\pi-\theta_-$	$\pi-\theta_+$
0.3	0.00	39.72	180.00	140.28
0.8	0.00	56.25	180.00	123.75
1.2	0.00	62.96	180.00	117.04
2.5	48.19	73.40	131.81	106.60

TABLE 4. Zones of silence above and below the shear layer.

Figure	Mach number	Thickness of shear layer	Angle of incidence (deg.)
5	0.3, 0.8, 1.2, 2.5	1	75
6	0.8	0, 0.1, 1, 10	75
7	0.8	1	60, 75, 120
8	2.5	1	15, 75, 165

TABLE 5. Acoustic fields on the shear layer.

one is positive and the other negative. The corresponding solutions

$$J_{\pm}(\zeta)=\sum_{n=0}^{\infty} f_n(\nu_{\pm})\zeta^{n+\nu_{\pm}}, \tag{63}$$

lead to wave fields

$$Q_{\pm}(y)=\sum_{n=0}^{\infty} f_n(\nu_{\pm})[1-\tanh(y/L)]^{n+\nu_{\pm}}, \tag{64}$$

which scale in the free stream (27*b*) as

$$Q_{\pm}(y\to\infty)\sim\zeta^{\nu_{\pm}}\sim \mathrm{e}^{-2\nu_{\pm}y/L}\sim\exp(y/L)\exp\left(\mp y\sqrt{1/L^2+k^2/4}\right), \tag{65}$$

so that Q_- diverges and Q_+ is evanescent.

A bounded acoustic field is thus of the form $Q_+(y)$, and for a shear layer has to be matched to (38):

$$Q_+(y)=A_-P^+(y)+B_-P^-(y). \tag{66}$$

The continuity of pressure and normal displacement at $y=0$ yields

$$\begin{bmatrix} J_+(0) \\ -J'_+(0) \end{bmatrix}=\begin{bmatrix} G_+(0) & G_-(0) \\ G'_+(0) & G'_-(0) \end{bmatrix}\begin{bmatrix} A_- \\ B_- \end{bmatrix}, \tag{67}$$

which determines uniquely the amplitude of the incident A_- and reflected B_- waves below the shear layer; this is the only case in which the sound field is bounded at the Mach condition above the shear layer, i.e. for all other values of (A_-, B_-) the acoustic field could be unbounded at the critical layer in the upper free stream.

4. Scattering coefficients and wave field in a shear layer

The preceding results could be used to plot the acoustic field in a number of cases, e.g. a shear layer (i) without a critical layer, (ii) with a critical layer in the upper free stream leading to radiation at the Mach condition or (iii) with a critical layer in the shear layer (table 1). For each of these cases could be plotted: (i) the reflection

and transmission coefficients, as a function of angle of incidence θ, for different free-stream Mach number M, and thickness of the shear flow on a wavelength scale δ; (ii) the amplitude and phase of the acoustic pressure, as a function of the transverse coordinate across the shear flow, for various combinations of θ, M, δ. The discussion concerns a selection of data from this vast range of possibilities.

4.1. *Effects of Mach number, angle of incidence and shear layer thickness*

The condition that sound can propagate in the upper free stream (54a, b), does not depend on the boundary layer thickness δ, but only on the Mach number, e.g. for the four Mach numbers, which includes low-subsonic, high-subsonic, transonic and supersonic free streams, the angles specifying the 'zones of silence' above and below the shear layer (figure 2a, b) are given in table 4.

The moduli and phases of the reflection and transmission coefficients are plotted as a function of angle of incidence in figure 3 for a single Mach number

$$M = 0.8. \quad \delta = 0, 0.1, 1, 10, \tag{68a, b}$$

and a vortex sheet and three progressively thicker shear layers, and in figure 4 for four Mach numbers and shear layer thickness equal to the wavelength

$$M = 0.3, 0.8, 1.2, 2.5, \quad \delta = 1. \tag{69a, b}$$

The modulus and phase of the acoustic pressure is plotted for four cases listed in table 5, which demonstrate the affects of the angle of incidence, the Mach number of the free streams, and the thickness of the shear layer measured on the scale of the wavelength in the free stream. In the cases of supersonic free streams, $M = 1.2, 2.5$, there is a critical layer in the shear layer. In this case it is necessary to match the solutions near the free streams (§ 2.3, § 3.1) to that near the critical layer (Campos & Kobayashi 2000*b*), using methods similar to those in § 3.2.

4.2. *Modulus and phase of the reflection and transmission coefficients*

The modulus of the reflection factor (figure 3*a*) is unity in the zone of silence $\theta < 56^\circ$ or $\theta > 124^\circ$ in table 4 for a free-stream Mach number $M = 0.8$. Propagation above and below the shear layer is possible only for the range of angles of incidence $56^\circ < \theta < 124^\circ$. In this range the modulus of the reflection coefficient for a vortex sheet $\delta = 0$ is zero for normal incidence $\theta = 90^\circ$ and then increases away from the vertical, being maximum at $\theta = 65^\circ, 115^\circ$, before decaying towards the edge of the zone of silence $\theta \leqslant 56^\circ$, or $\theta \geqslant 124^\circ$, where it becomes unity. For a thin shear layer, e.g. thickness one-tenth of the wavelength $\delta = 0.1$, there is still noticeable wave reflection, but for thicker shear layers $\delta = 1, 10$ the modulus of the reflection coefficient is practically zero in the range of angles of incidence corresponding to propagation on both sides of the shear layer.

The phase of the reflection coefficient (figure 3*b*) is either 0 or π for a vortex sheet $\delta = 0$, and is more rounded-off for a thin shear layer $\delta = 0.1$. For a shear layer of thickness equal to the wavelength $\delta = 1$ the phase of the reflection coefficient is significant, and it becomes small for a thick shear layer $\delta = 10$. The modulus of the transmission coefficient (figure 3*c*) differs little between a vortex sheet and a shear layer, and is weakly dependent on the thickness of the latter. The modulus of the transmission coefficient is unity ($|T| = 1$) for normal incidence $\theta = 90^\circ$, and is smaller ($|T| < 1$) in the forward arc $\theta < 90^\circ$, larger ($|T| > 1$) in the rear arc $\theta > 90^\circ$, except near to the zone of silence; $|T| \to \infty$ for $\theta \to \theta_+$ because the wave field below the shear layer is evanescent, and $|T| \to 0$ for $\theta \to \pi - \theta_+$ because above the shear layer

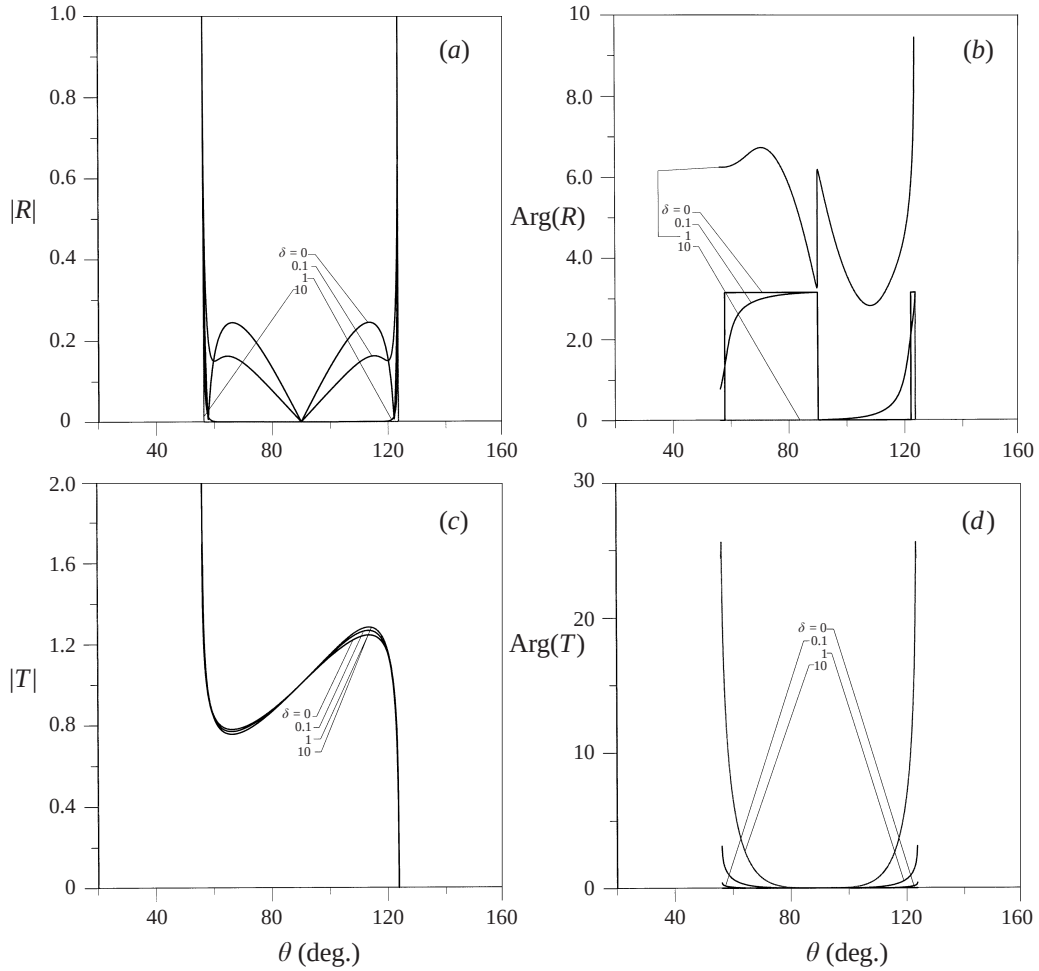

FIGURE 3. (a, c) Modulus and (b, d) phase of the reflection and transmission coefficients, versus angle of incidence θ, for free-stream Mach numbers $M = 0.8$, and a vortex sheet $\delta = 0$, and a shear layer of thickness $\delta = 0.1, 1, 10$ on the scale of a wavelength.

the sound field is evanescent. The phase of the transmission coefficient (figure 3*d*) is small over most of the range of angles of incidence for propagating waves on both sides of the shear layer, and diverges as evanescence conditions are approached at the edge of the 'zones of silence'.

Considering (figure 4) a shear layer of thickness equal to the wavelength and several free-stream Mach numbers (69*a, b*) the modulus of the reflection coefficient is unity in the 'zones of silence' and zero in the propagation zone (table 4), with a sharp transition in between (figure 4*a*). The phase of the reflection coefficient varies with the angle of incidence in the propagation zone, with a phase jump of π across normal incidence (figure 4*b*). The modulus of the transmission coefficient is unity for normal incidence, larger in the real arc and smaller in the forward arc, the effect being more pronounced for larger free stream Mach number (figure 4*c*). The phase of the transmission factor is small in the propagation zone, and diverges at the edges of the zones of silence, where the modulus of the transmission factor tends to zero (rear zone of silence) or diverges (forward zone of silence) (figure 4*d*).

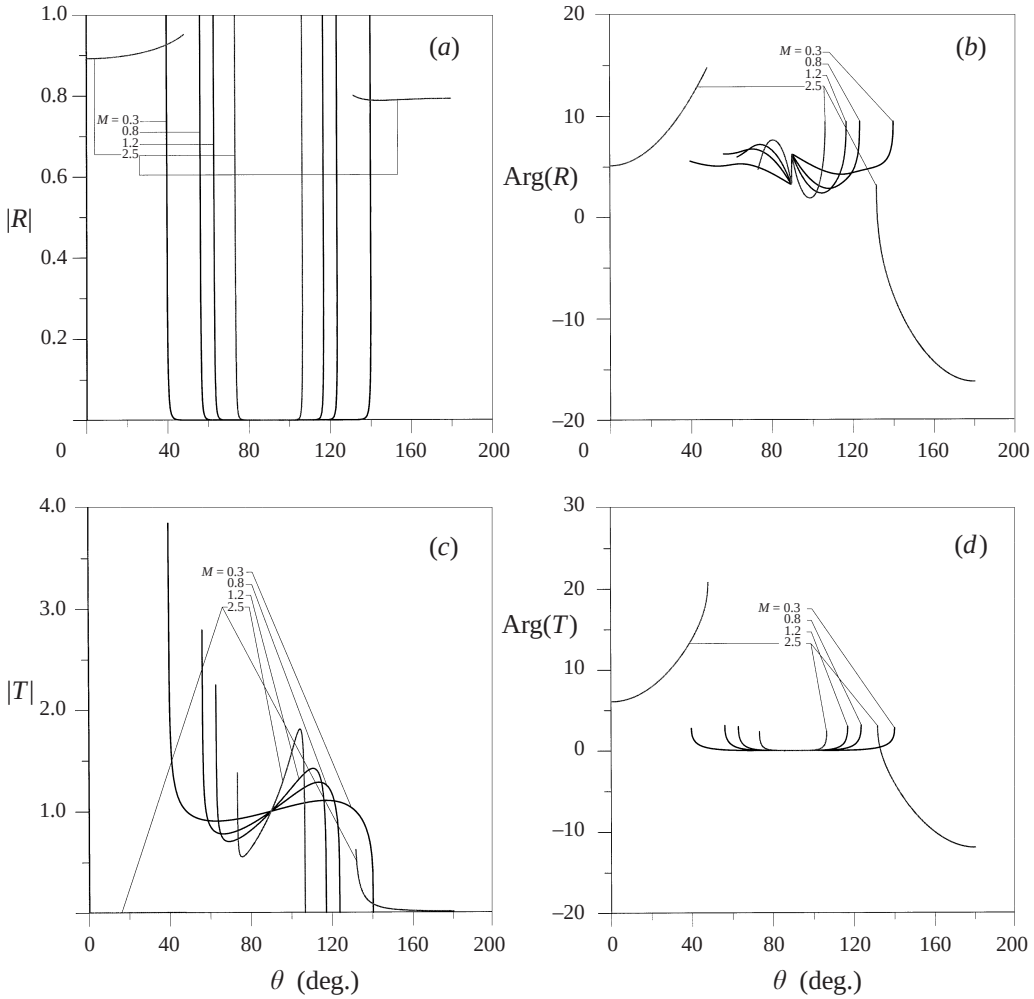

FIGURE 4. As figure 3, but for a shear layer of thickness equal to the wavelength $\delta = 1$, and four free-stream Mach numbers corresponding to low-subsonic $M = 0.3$, high-subsonic $M = 0.8$, transonic $M = 1.2$ and supersonic $M = 2.5$ jets.

4.3. *Modulus and phase of acoustic pressure in the shear layer*

The modulus and phase of the acoustic pressure,

$$P = |P| \exp\{\mathrm{i} \arg(P)\}, \quad -4 \leqslant Y \equiv y/L \leqslant 4, \tag{70a,b}$$

are plotted next versus distance across the shear layer, made dimensionless by dividing by the shear layer thickness L. The same four free-stream Mach numbers and shear layer thickness (table 5) are considered (figure 5), for an angle of incidence $\theta = 75^\circ$ corresponding to propagation on both sides of the shear layer in all cases (table 4). The modulus of the acoustic pressure (figure 5*a*) decays more as it crosses the shear layer for larger Mach number; in the case of supersonic free streams there are visible amplitude oscillations at the lower but not in the upper stream. The phase of the acoustic pressure (figure 5*b*) has a comparable total variation across the shear layer for all Mach numbers, but is close to a linear function of thickness for low subsonic

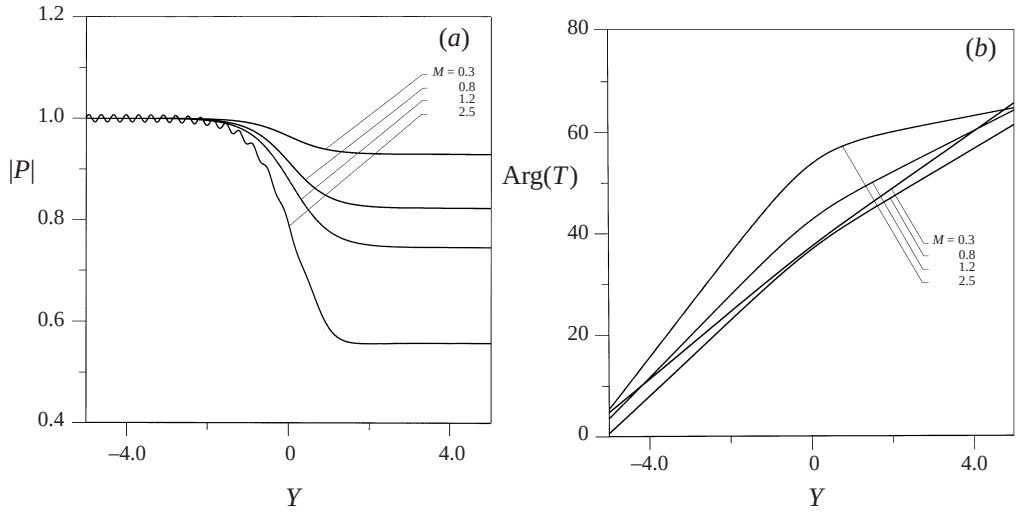

FIGURE 5. (*a*) Modulus and (*b*) phase of acoustic pressure (70*a*) versus distance across the shear layer normalized to shear layer thickness (70*b*), for a shear layer of thickness equal to the wavelength, and angle of incidence $\theta = 75°$ in the propagation zone (table 4) for all four free-stream Mach numbers.

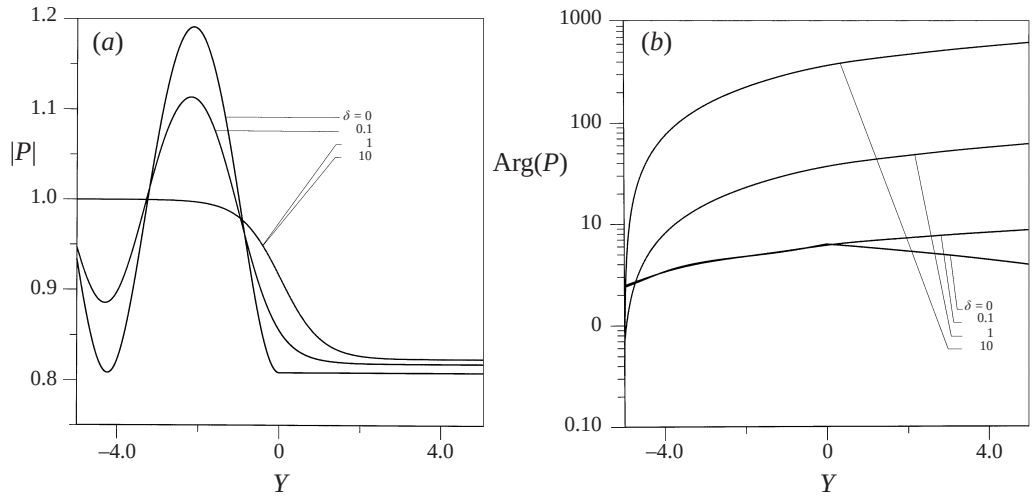

FIGURE 6. As figure 5, but for a high subsonic free-stream Mach number $M = 0.8$, and a vortex sheet $\delta = 0$ and shear layers of various thicknesses on a wavelength scale $\delta = 0.1, 1, 10$.

free streams, and has a noticeable 'kink' for the supersonic free streams, i.e. it varies more rapidly in the lower half than in the upper half of the shear layer.

Retaining the angle of incidence, for high-subsonic free jets (table 5) the effect of the thickness of the shear layer (figure 6) is significant both in the modulus and phase of the acoustic pressure. The modulus of the acoustic pressure (figure 6*a*) decays smoothly for the thick shear layer $\delta = 1, 10$; for the vortex sheet $\delta = 0$ and thin shear layer $\delta = 0.1$, it oscillates in the lower half of the shear layer and becomes constant in the upper half. The phase of the acoustic pressure (figure 6*b*) increases rapidly in the lower half of the shear layer (upstream propagation), more noticeably for thicker

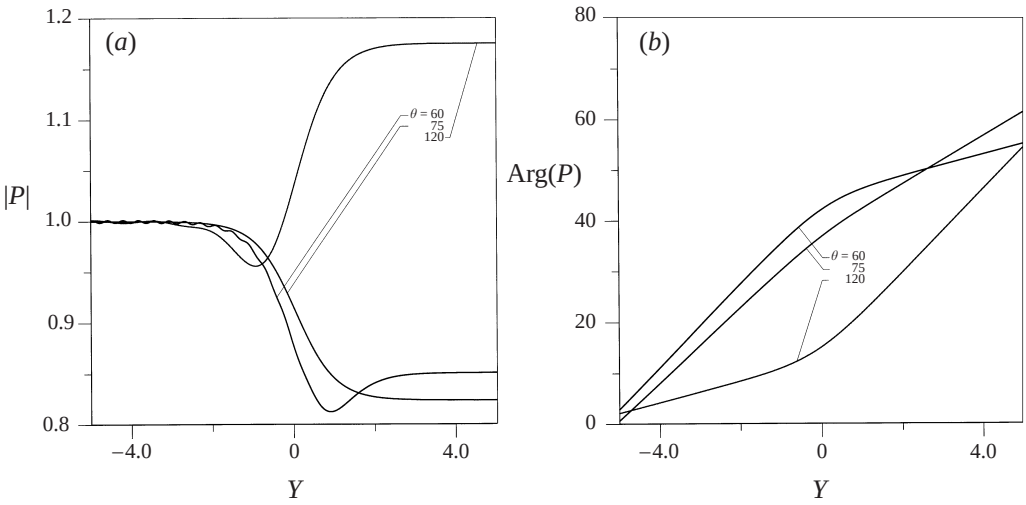

FIGURE 7. As figure 6, but for a shear layer of thickness equal to the wavelength $\delta = 1$, and three angles of incidence in the propagation zone $56^\circ < \theta < 124^\circ$, two in the forward arc $\theta = 60, 75^\circ$ and one in the rear arc $\theta = 120^\circ$.

shear layers; it then tends to a constant value in the upper half of the shear layer (downstream propagation), with a larger value for thicker shear layers.

For the same shear layer (table 5) three angles of incidence are considered (figure 7) all in the propagation zone $56^\circ < \theta < 124^\circ$ in (table 4). The modulus of the acoustic pressure (figure 7*a*) shows a decay or attenuation for angles of incidence $\theta = 60^\circ, 75^\circ$ corresponding to downstream propagation ($\theta < 90^\circ$) in the upper free stream, and an increase or amplification for the angle of incidence $\theta = 120^\circ$ corresponding to upstream propagation in the upper free stream. The phase of the acoustic pressure (figure 7*b*) has a comparable total variation across the shear layer in all three cases, with an 'upward' kink for incidence in the forward arc $\theta < 90^\circ$ and a downward 'kink' for incidence in the rear arc.

5. Discussion

The final case of a shear layer with the same thickness (table 5) of the supersonic free streams (figure 8) is considered for angles of incidence (table 4) in the forward $\theta = 15^\circ$, central $\theta = 75^\circ$, and rear $\theta = 165^\circ$ propagation zones. The modulus of the acoustic pressure (figures 8*a*) decays smoothly across the shear layer in the central propagation zone $\theta = 75^\circ$. In the forward and rear propagation zones, $\theta = 15^\circ, 165^\circ$, the modulus of the acoustic pressure oscillates strongly in the lower half of the shear layer, and almost vanishes in the upper half of the shear layer; this is typical of the transition from 'light' to 'shadow', in the present case for sound rather than electromagnetic waves. The oscillations in the amplitude of the acoustic pressure (in figures 8*a*, as well as 5*a* and 7*a*) are due to reflection in the shear layer; the acoustic fields are calculated from multiple scattering series like (28*b*) and (39), consisting of an unidirectional wave as the leading term, plus multiple reflections of all orders in the following terms of the series.

The phase of the acoustic pressure (figure 8*b*) has a smaller total variation across the shear layer for incidence in the central propagation zone, $\theta = 75^\circ$, than in forward or rear propagation zones, $\theta = 15^\circ, 165^\circ$. In the central propagation zone, $\theta = 75^\circ$,

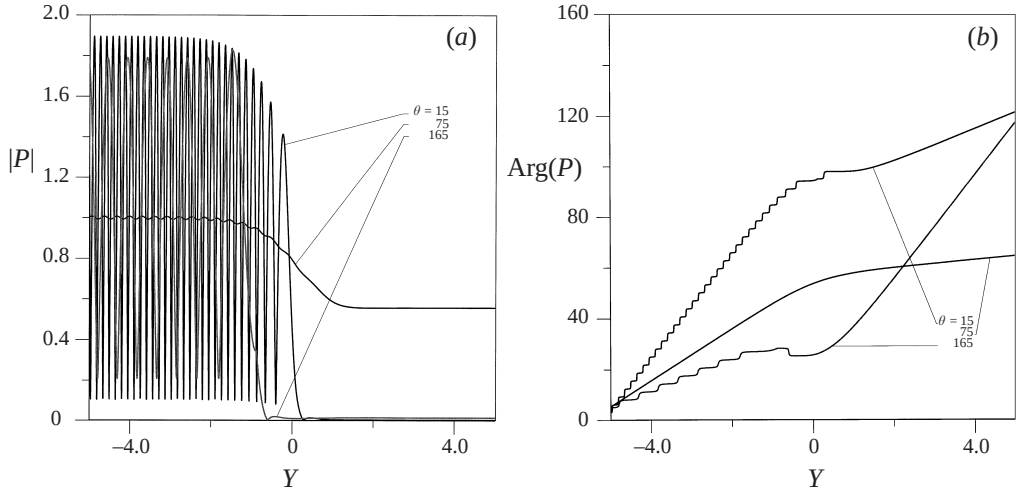

FIGURE 8. As figure 7, but for supersonic free streams $M = 2.5$, and angles of incidence in the forward $\theta = 15°$, central $\theta = 75°$ and rear $\theta = 165°$ propagation zones.

the phase is almost a linear function of the thickness of the shear layer, with a larger slope in the lower half (propagation upstream) than in the upper half (propagation downstream), resulting in a 'kink' near the layer of zero velocity. The total phase change across the shear layer is comparable for the angles of incidence in the forward $\theta = 15°$ and rear $\theta = 165°$ propagation zones; in both cases there are phase jumps of π at the nodes of the amplitude (in figure 8*a*). The phase curves have opposite 'kinks', i.e. upward in the forward propagation zone $\theta = 15°$ and downward in the rear propagation zone $\theta = 165°$, due to the opposite sequences, namely propagation upstream in the lower half and downstream in the upper half of the shear layer in the former case $\theta = 15°$, and vice versa in the latter case $\theta = 165°$.

The properties of the acoustic fields in a shear layer which have been demonstrated include the following: (i) a vortex sheet reflects sound waves much more strongly than a shear layer of moderate thickness $\delta \geqslant 1$ on a wavelength scale; (ii) the difference between the vortex sheet and shear layer is less marked for the transmission coefficient; (iii) the interaction between sound and flow in a shear layer is much more complex, and richer in physical phenomena, than for a vortex sheet. Thus the vortex sheet (Miles 1958) is an acceptable idealization of a shear layer only for thickness less than about a tenth of the wavelength. The other simple idealization is the opposite limit of sound 'rays'; here the wavelength should be much smaller than the thickness of the shear layer (Amiet 1978). Between these opposite extremes, and most notably for wavelengths comparable to the thickness of the shear layer, the acoustic fields in the latter are specified by the solution of the wave equation. The method of exact solution of the wave equation applies not only to the propagation of sound in a shear layer (as the main subject of the paper), but also to the triggering of its instabilities (as outlined in Appendix A).

Appendix A. Acoustic triggering of instabilities in a shear flow

The denominator of the reflection R and transmission T coefficients is the function in square brackets on the left-hand side of (45):

$$F_+(1)G'_-(1) + F'_+(1)G_-(1) \equiv H(kL, \omega L/c, M), \tag{A 1}$$

which depends on three dimensionless parameters: the Mach number (14*b*) and the dimensionless horizontal wavenumber (11*b*) and frequency (11*a*). For real wavenumber k and frequency ω the function H in (A 1) does not generally vanish, and the scattering coefficients R, T in (45) remain finite; this is the case addressed in the main paper, of sound propagation in a shear flow, without triggering instabilities. The case where instabilities are triggered, which will be mentioned briefly in this Appendix, corresponds to singular scattering coefficients in (45), or the vanishing of (A 1), which generally occurs only for complex k or ω, leading to two cases. In case 1 of real wavenumber k, the roots of

$$0 = H(kL, (\omega_r + \mathrm{i}\omega_i)L/c, M) \tag{A 2}$$

specify a complex frequency:

$$\omega = \omega_r + \mathrm{i}\omega_i: \quad \exp(-\mathrm{i}\omega t) = \exp(-\mathrm{i}\omega_r t)\exp(\omega_i t), \tag{A 3}$$

whose imaginary part is the rate of growth in time, and generally depends on the Mach number and dimensionless wavenumber:

$$H = 0: \quad \omega_i = (c/L) f(kL, M). \tag{A 4}$$

The boundary between the condition of temporal growth $\omega_i > 0$ or decay $\omega_i < 0$ of disturbances is $\omega_i = 0$, and specifies a relation

$$\omega_i = 0: \quad k = L^{-1} g(M), \tag{A 5}$$

between wavenumber and Mach number, which is the 'stability boundary'.

An alternative approach is case II of real frequency ω, and complex wavenumber root of the corresponding equation:

$$0 = H((k_r + \mathrm{i}k_i)L, \omega L/c, M), \tag{A 6}$$

which specifies

$$k = k_r + \mathrm{i}k_i: \quad \exp(\mathrm{i}kt) = \exp(\mathrm{i}k_r t)\exp(-k_i t), \tag{A 7}$$

with spatial growth for $k_i < 0$ and decay for $k_i > 0$ in

$$H = 0: \quad k_i = L^{-1} \bar{f}(\omega L/c, M), \tag{A 8}$$

so that the 'stability boundary' corresponds to:

$$k_i = 0: \quad \omega = (c/L)\bar{g}(M). \tag{A 9}$$

In either case I or II, the calculation of the acoustic pressure from its spectrum, leads to the evaluation of a Fourier integral (5), with the function (A 1) in the denominator. Thus the instabilities of the shear flow, which are specified by the roots of the function (A 1), appear as poles of the integrand in (5); the residues at these poles specify the acoustic field triggered by these instabilities, by suitable deformation of the path of integration away from the real axis, or by closing it with a suitable contour. The choice of path of integration depends on the location of the poles, and thus on the roots of (A 1), which are specified by the Frobenius–Fuchs series (24*b*), (25*a*), (26), (32), (33), (35). Although it is not the purpose of the present paper to go in detail into the study of instabilities of a shear flow, some remarks will be made on the calculation of these Frobenius–Fuchs series, since they are the same as used to calculate sound scattering by a shear flow, in the main body of the paper.

Appendix B. Rate of convergence and truncation of Frobenius–Fuchs series

Both for the case of sound propagation across a shear layer (main paper) and the triggering of instabilities of a shear flow (Appendix A), the acoustic fields are calculated from Frobenius–Fuchs series, which are power series:

$$Q(z) = \sum_{n=0}^{\infty} q_n z^{n+\sigma}, \tag{B 1}$$

where the index σ is a constant, and the coefficients q_n satisfy a linear recurrence formula of order m:

$$q_n = r_1 q_{n-1} + r_2 q_{n-2} + \cdots + r_m q_{n-m}. \tag{B 2}$$

The rate of convergence is defined as the ratio of two successive terms of the series:

$$|q_n z^{n+\sigma}|/|q_{n-1} z^{n+\sigma-1}| = |z||q_n/q_{n-1}| \equiv s, \tag{B 3}$$

and if it is known an upper bound for the truncation error after n terms follows:

$$E_n = \left| \sum_{j=n}^{\infty} q_j z^{\sigma+j} \right| \leqslant |z|^{\sigma+n} |q_n| \sum_{j=0}^{\infty} s^j = \frac{|z|^{\sigma+n}|q_n|}{1-s}. \tag{B 4}$$

In the case of a binary recurrence formula

$$m = 1: \quad q_n = r q_{n-1}, \tag{B 5}$$

the rate of convergence (B 3) follows immediately

$$s = |z| \lim_{n\to\infty} r \equiv |z| r^{\infty}. \tag{B 6}$$

This is the case for the most usual special functions (Bessel, Hypergeometric, etc.).

In the present problem the simplest recurrence formula is triple:

$$q_n = r_1 q_{n-1} + r_2 q_{n-2}, \tag{B 7}$$

i.e. in the case (60) of acoustic waves at the Mach condition

$$q_n \equiv f_n: \quad r_1 = \frac{2(n+\nu-1)(2n+2\nu-3)}{4(n+\nu)(n+\nu-2)-k^2} \to 1 \equiv r_1^{\infty}, \tag{B 8a}$$

$$n \to \infty: \quad r_2 = -\frac{(n+\nu-2)(n+\nu-3)+\Omega^2}{4(n+\nu)(n+\nu-2)-k^2} \to -\frac{1}{4} \equiv r_2^{\infty}, \tag{B 8b}$$

where the limits are taken as $n \to \infty$. In the case of a triple recurrence formula, the rate of convergence can be calculated from the continued fraction:

$$q_n/q_{n-1} = r_1 + r_2/(q_{n-1}/q_{n-2}): \quad \lim_{n\to\infty} q_n/q_{n-1} = r_1^{\infty} + \cfrac{r_2^{\infty}}{r_1^{\infty} + \cfrac{r_2^{\infty}}{r_1^{\infty} + \cfrac{r_2^{\infty}}{r_1^{\infty} + \cfrac{r_2^{\infty}}{\cdots}}}} \tag{B 9}$$

where $r_i^{\infty} \equiv \lim_{n\to\infty} r_i, i = 1, 2$. In the present case $z \equiv \zeta$ in (57a), and thus the rate of convergence is given by

$$s = \frac{|\zeta|}{2}, \tag{B 10}$$

because the continued fraction (B 9) with the values (B8a, b) converges to $1/2$, as will be shown next.

The continued fraction (B 9) is equivalent to the discrete mapping

$$x_n = h(x_{n-1}), \tag{B 11}$$

where the function h is defined by

$$h(x) = r_1^\infty + r_2^\infty / x. \tag{B 12}$$

The equation (B 11) converges to a fixed point $\bar{x}$ such that

$$\lim_{x\to\infty} x_n = \bar{x}: \quad \bar{x} = r_1^\infty + r_2^\infty/\bar{x}. \tag{B 13}$$

The quadratic equation (B 13) has roots specifying the fixed points:

$$2\bar{x} = r_1^\infty \pm \sqrt{(r_1^\infty)^2 + 4r_2^\infty}. \tag{B 14}$$

For the values (B8a, b) the roots (B 14) coincide $\bar{x} = 1/2$, so that there is only one fixed point; this is the limit of (B 9) used in (B 10).

The solution in all the remaining cases (24b), (25a) and (32), (33) are given by quadruple recurrence formulas:

$$q_n = r_1 q_{n-1} + r_2 q_{n-2} + r_3 q_{n-3}, \tag{B 15}$$

e.g. for (25a)

$$q_n \equiv a_n: \quad r_0 = (1-\Lambda)[4(n+\sigma)^2 + k_+^2 L^2], \tag{B 16a}$$

$$r_1 = r_0^{-1}\{2(n+\sigma-1)[2(1-2\Lambda)(n+\sigma-2)+3-\Lambda] - \Lambda[k_+^2 L^2 + 2\Omega^2(1-\Lambda)^2]\}, \tag{B 16b}$$

$$r_2 = -r_0^{-1}\{(n+\sigma-2)[(1-5\Lambda)(n+\sigma-3)+2] + 3\Omega^2\Lambda^2(1-\Lambda)\}, \tag{B 16c}$$

$$r_3 = -r_0^{-1}\Lambda\{(n+\sigma-3)(n+\sigma-4) + \Omega^2\Lambda^2\}, \tag{B 16d}$$

implying that

$$r_1 \to (1-2\Lambda)/(1-\Lambda) \equiv r_1^\infty, \quad r_2 \to (5\Lambda-1)/[4(1-\Lambda)] \equiv r_2^\infty, \quad r_3 \to -\Lambda/[4(1-\Lambda)] \equiv r_3^\infty. \tag{B 17a, b, c}$$

as $n \to \infty$. In the case of small Λ

$$5\Lambda \ll 1: \quad r_1 \to 1, \quad r_2 \to -1/4, \quad r_3 \to r_3^\infty \ll -1/20, \tag{B 18a, b, c}$$

if the q_n are decreasing, then (B 15) can be approximated by a triple recurrence formula (B 7), and the preceding method applies again.

If Λ is not small, the preceding approximation does not apply. In this case to compute the rate of convergence the quadruple recurrence formula (B 15) is written as

$$l_n = q_n/q_{n-1}: \quad l_n = r_1 + r_2/l_{n-1} + r_3/(l_{n-1}l_{n-2}), \tag{B 19}$$

leading to the limit

$$l = \lim_{n\to\infty} l_n: \quad l = r_1^\infty + r_2^\infty/l + r_3^\infty/l^2, \tag{B 20}$$

which specifies the fixed points as roots of the cubic

$$0 = l^3 - r_1^\infty l^2 - r_2^\infty l - r_3^\infty = \left(l - \frac{1}{2}\right)^2 \left(l + \frac{\Lambda}{1-\Lambda}\right), \tag{B 21}$$

where (B 17a, b, c) were used. It follows that the rate of convergence is specified by

$$s = \max\left(\frac{1}{2}, \frac{\Lambda}{\Lambda - 1}\right)|\zeta|. \tag{B 22}$$

This result shows that the radius of convergence of the Frobenius–Fuchs series is, in this case, equal to min $(2, (\Lambda - 1)/\Lambda)$. It also shows that the rate of convergence s increases linearly with $|\zeta|$. Thus, the series can be summed with as many terms as needed to have a given number of accurate digits (four in the calculation for the plots in figures 3 to 8). Given ζ, the rate of convergence s is calculated from equation (B 22), and then used in equation (B 4) as an error estimation (in actual computations ten successive terms are compared, in order to overcome some oscillations in the convergence of the terms of the series). Also, by changing the matching point within the region of convergence of each series, it can be verified that the acoustic fields are not sensitive to this choice, except very close to the boundaries of the region of convergence.

REFERENCES

Almgren, G. 1976 Acoustic boundary layer influence in scale model simulation of sound propagation. *J. Sound Vib.* **105**, 321–327.

Amiet, R. K. 1978 Refraction of sound by a shear layer. *J. Sound Vib.* **58**, 467–482.

Balsa, T. F. 1976*a* The far-field of high-frequency convected, singularities in sheared flows, with application to jet noise prediction. *J. Fluid Mech.* **74**, 193–208.

Balsa, T. F. 1976*b* Refraction and shielding of sound from a source in a jet. *J. Fluid Mech.* **76**, 443–456.

Campos, L. M. B. C. & Kobayashi, M. H. 2000*a* On the propagation of sound in an non-isothermal shear flow. (In preparation.)

Campos, L. M. B. C. & Kobayashi, M. H. 2000*b* On the scattering of sound by a boundary layer (In preparation.)

Campos, L. M. B. C., Oliveira, J. M. G. & Kobayashi, M. H. 1998 On sound propagation in a linear shear flow. *J. Sound Vib.* **95**, 739–770.

Campos, L. M. B. C. & Serrão, P. G. T. A. 1999 On the acoustics of an exponential boundary layer. *Phil. Trans. R. Soc. Lond.* A **356**, 2335–2378.

Drazin, P. G. & Reid, W. H. 1979 *Hydrodynamic Stability*. Cambridge University Press.

Ffowcs Williams, J. E. 1974 Sound production at the edge of a steady flow. *J. Fluid Mech.* **66**, 791–816.

Goldstein, M. 1979 Scattering and distortion of the unsteady motion on transversely sheared mean flows. *J. Sound Vib.* **91**, 601–602.

Goldstein, M. 1982 High-frequency sound emission from multipole sources embedded in arbitrary transversely sheared mean flows. *J. Sound Vib.* **80**, 449–460.

Goldstein, M. & Rice, E. 1973 Effect of shear on duct wall impedance. *J. Sound Vib.* **30**, 79–84.

Graham, E. W. & Graham, B. B. 1968 Effect of a shear layer on plane waves in a fluid. *J. Acoust. Soc. Am.* **46**, 169–175.

Hanson, D. B. 1984 Shielding of propfan cabin noise by the fuselage boundary layer. *J. Sound Vib.* **92**, 591–598.

Haurwitz, W. 1932 Zur Theorie der Wellenbewegungen in Luft and Wasser. *Veroff. Geophys. Inst. Univ. Leipz.* **6**, 334–364.

Jones, D. S. 1977 The scattering of sound by a simple shear layer. *Phil. Trans. R. Soc. Lond.* A **284**, 287–328.

Jones, D. S. 1978 Acoustics of a splitter plate. *J. Inst. Math. Applics.* **21**, 197–209.

Kamke, E. 1944 *Differentialgleichungen*, vols 1 and 2. Teubner.

Koutsoyannis, S. P. 1979 Characterization of acoustic disturbances in linearly sheared flows. *J. Sound Vib.* **68**, 187–202.

Koutsoyannis, S. P., Karamchti, K. & Galant, D. C. 1980 Acoustic resonances and sound scattering by a shear layer. *Am. Inst. Aeron. Astron. J.* **18**, 1446–1450.

KÜCHEMAN, D. 1938 Störungebewegungen in einer Gasströmung mit Grenzschicht. *Z. Angew. Math Mech.* **30**, 79–84.

LIN, C. C. 1955 *Hydrodynamic Stability Theory*. Cambridge University Press.

MICHALKE, A. 1965 On spatially growing disturbances in an inviscid shear layer. *J. Fluid Mech.* **23**, 521–544.

MICHALKE, A. 1984 Survey on jet instability theory. *Prog. Aerospace Sci.* **21**, 159–199.

MICHALKE, A. 1989 On the propagation of sound generated in a pipe of circular cross-section with uniform mean flow. *J. Sound Vib.* **134**, 203–234.

MICHALKE, A. & TIMME, A. 1967 On the inviscid instability of certain two-dimensional vortex-type flows. *J. Fluid Mech.* **29**, 647–666.

MILES, J. M. 1958 On the disturbed motion of a vortex sheet. *J. Fluid Mech.* **4**, 538–554.

MÖHRING, W., MULLER, E. A. & OBERMEIER, F. 1983 Problems in flow acoustics. *Rev. Mod. Phys.* **55**, 707–724.

MYERS, M. K. & CHUANG, S. L. 1983 Uniform asymptotic approximations for duct acoustic modes in a thin boundary-layer flow. *Am. Inst. Aeron. Astron. J.* **22**, 1234–1241.

NAYFEH, A. H., KAISER, J. E. & TELIONIS, D. P. 1975 Acoustics of aircraft engine-duct systems. *Am. Inst. Aeron. Astron. J.* **13**, 130–153.

PRIDMORE-BROWN, D. C. 1958 Sound propagation in a fluid flowing through an attenuating duct. *J. Fluid Mech.* **4**, 393–406.

RONVEAUX, A. (Ed.) 1996 *Heun's Differential Equation*. Oxford University Press.

SCOTT, J. N. 1979 Propagation of sound waves through a linear shear layer. *Am. Inst. Aeron. Astron. J.* **17**, 237–245.